Protein Functionalities

DOI: 10.1002/ange.201007824

Inhibition of Amyloid Peptide Fibrillation by Inorganic Nanoparticles: Functional Similarities with Proteins**

*Seong Il Yoo, Ming Yang, Jeffrey R. Brender, Vivekanandan Subramanian, Kai Sun, Nam Eok Joo, Soo-Hwan Jeong, Ayyalusamy Ramamoorthy, and Nicholas A. Kotov**

Aβ fibrils (or Abeta nanowires, NWs) have been implicated in many neurodegenerative disorders such as Alzheimer disease (AD).[1] Both soluble oligomers and mature fibrils from Aβ are neurotoxic and cause death of brain cells.[1–3] The inhibition of Aβ assembly has been considered as the primary therapeutic strategy for the neurodegenerative diseases. Short peptides, in particular KLVFF residues, have been designed to interfere with β-structured aggregation through hydrophobic interactions.[4,5] Proteins capable of binding to Aβ also have an inhibitory effect on Aβ fibrillation.[4,6] Recently, antibodies against Aβ as well as surface-modified proteins with Aβ residues have been applied to prevent Aβ aggregation and reduce the toxicity.[4,7] Although peptide or protein analogues with specific binding sites might have the primary importance for fundamental studies and diagnostics of the neurodegenerative disorders, therapeutic agents have not been developed within this strategy. Some of the problems are the blood–brain barrier permeability,[4,8] the complexity of their synthesis, the low in vivo stability, and the low efficacy which can be attributed in part to the fact that these agents are designed to bind to peptide monomers in a 1:1 ratio.[1d,4,5,9]

Considering the fact that many NPs are capable of self-organization into structures similar to those of Aβ peptides,[10] it is intriguing to investigate the nexus of self-organization processes between NPs and peptides especially because the assembly behavior of NPs reveals similarities with those of biological species. Such studies have mostly fundamental importance but may also reveal new aspects of NP toxicology and provide alternative methodology for preventing the agglomeration of Aβ peptides.[11] Although not all NPs are biocompatible, they might be worth some consideration as therapeutic agents because they are easy to synthesize and have great in vivo stability. In this respect, the nonbiodegradable nature of inorganic NPs can be of potential advantage and can help to fully utilize their activity over a long period of time. Many NPs can also penetrate the blood–brain barrier, which further substantiates our interest in them in conjunction with amyloid fibrillation in brain tissue.

The existing data on the effects of both organic and inorganic NPs on peptide assembly are controversial. Overall, the presence of NPs has typically promoted aggregation of Aβ, which was explained in terms of a condensation-ordering mechanism.[12] Since the fibrillation occurs by nucleation-dependent kinetics, the increased local concentration of peptides in the vicinity of NPs as a result of electrostatic attraction greatly accelerates the fibril formation. For example, copolymeric NPs of *N*-isopropylacrylamide and *N*-*tert*-butylacrylamide with diameters of 70 and 200 nm, cerium oxide NPs with a diameter of 16 nm, polymer-coated quantum dots with a diameter of 16 nm, and carbon nanotubes catalyzed the fibrillation of the amyloid protein of β_2 microglobulin.[12b] Similarly, the strong absorption capacity of TiO_2 NPs (20 nm in diameter) to the amyloid peptide promoted fibril formation.[12c] Also, it was further reported that biological molecules,[13a,b] large colloidal particles,[13c] and liquid–air and liquid–solid interfaces[13d,e] promote the fibril formation as well. At the same time, some polymeric NPs (40 nm in diameter) have been found to slow down the rate of Aβ fibrillation by depleting the amount of free monomeric peptides, although the fibril formation still could not be prevented.[14a] Surface-modified nanogels with a diameter of 14 nm,[14b] micelles,[14c] and fullerenes[14d] were able to alter the conformation of the peptides and reduce the toxic activity. *N*-acetyl-L-cysteine-capped quantum dots with a diameter of 3–5 nm also displayed inhibitory activity towards fibrillation which was attributed to the formation of hydrogen bonds,[14e] albeit the same bonds are also involved in peptide–NP

[*] Dr. M. Yang, Prof. N. A. Kotov
Department of Chemical Engineering, Materials Science and Biomedical Engineering, University of Michigan
Ann Arbor, MI 48109 (USA)
E-mail: kotov@umich.edu
Prof. S. I. Yoo
Department of Chemical Engineering, University of Michigan
Ann Arbor, MI 48109 (USA)
and
Department of Polymer Engineering
Pukyong National University, Busan 608-739 (Republic of Korea)
Dr. J. R. Brender, Dr. V. Subramanian, Prof. A. Ramamoorthy
Department of Chemistry and Biophysics
University of Michigan, Ann Arbor, MI 48109 (USA)
Dr. K. Sun
Department of Materials Science and Engineering
University of Michigan, Ann Arbor, MI 48109 (USA)
Dr. N. E. Joo
Department of Periodontics and Oral Medicine
School of Dentistry, University of Michigan
Ann Arbor, MI 48109 (USA)
Prof. S.-H. Jeong
Department of Chemical Engineering
Kyoungpook National University, Daegu 702-701 (Korea)

[**] This work was supported by the NSF (grant numbers 0932823, 0933384, and 0938019), the NIH (grant numbers 1R21CA121841-01A2 and 5R01EB007350-02), and in part by the DARPA (grant number W31P4Q-08-C-0426). S.I.Y. acknowledges the support of the Korea Research Foundation (grant number KRF-2008-357-D00078).

Supporting information for this article is available on the WWW under http://dx.doi.org/10.1002/anie.201007824.

systems which promote assembly of amyloid peptides. The formation of dense NP coatings on fibrils was observed and the computer model of a kinetic model based on nucleation and growth inhibition was discussed.[14e]

Focusing on finding an efficient fibrillation inhibitor as the most challenging task, we need to admit that there is barely any clarity about what forces are to be engaged and what nanomolecular scale species are preferential for this purpose. As a new step in this direction, we report here the strong inhibition of Aβ fibrillation by TGA (thioglycolic acid)-stabilized CdTe NPs. These NPs were originally selected because they generally resemble some proteins in terms of the size, charge, and association behavior (Figure 1 a).[15] We

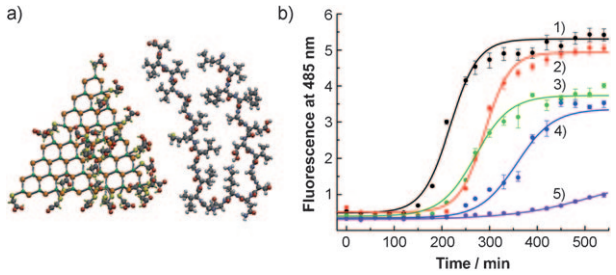

Figure 1. a) Molecular structure of CdTe NPs and $A\beta_{1\text{-}42}$ peptide. Some of the TGA molecules adsorbed to the surface of the CdTe NPs are removed for clarity. The peptide is folded in the configuration that is characteristic for the fibrils. Molecular modeling was carried out by SPARTAN. b) Kinetics of $A\beta_{1\text{-}40}$ fibrillation with and without CdTe NPs. Time-dependent ThT fluorescence was monitored at 485 nm with an excitation wavelength of 450 nm. The [CdTe]/[$A\beta_{1\text{-}40}$] molar ratio was varied from 0 to 0.005: 1) 0, 2) 0.001, 3) 0.005, 4) 0.01 and 5) 0.05. The fluorescence intensity of ThT at 485 nm is proportional to the amount of fibrils.

reasoned that it is possible that a minor fraction of NPs would have the proper local geometry and conformation of stabilizers to specifically self-assemble with (mis)folded peptides that can either accelerate or frustrate the fibrillation. The eventual mechanism of NP–peptide interaction was found to be markedly different from the one that we envisioned and from those considered previously for any kind of NPs[12,14] but very similar to that found for protective proteins inhibiting peptide fibrillation in the body.[6]

To examine the influence of CdTe NPs on the fibril formation of amyloid-β peptides consisting of 40 residues (denoted as $A\beta_{1\text{-}40}$ hereafter), incubation solutions of the $A\beta_{1\text{-}40}$ with and without NPs were prepared. The kinetics of fibrillation can be monitored by a dye-binding assay with thioflavin T (ThT), the fluorescent spectrum of which can be altered with the growth of fibrils (Figure 1 b).[12b,c,14a] As for the neat peptide (Figure 1 b, trace 1), the fibrillation follows a conventional nucleated-growth mechanism which can be described by a lag phase, a rapid exponential growth, and a final equilibrium state. Accordingly, the experimental data were fitted by a sigmoidal equation (solid lines) to extract kinetic constants.[16]

When the NPs were introduced (Figure 1 b, traces 2–5), the fluorescence intensity at saturation gradually decreased with the increase of the [CdTe]/[$A\beta_{1\text{-}40}$] molar ratio, indicating consistent inhibition of fibrillation in a dose-dependent manner by CdTe NPs. At the same time, the lag phase was extended from 159.5 minutes for the pure peptide to 236.3, 197.5, and 279.9 minutes for [CdTe]/[$A\beta_{1\text{-}40}$] molar ratios of 0.001, 0.005, and 0.01, respectively. The lag time for the case of [CdTe]/[$A\beta_{1\text{-}40}$] = 0.05 (Figure 1 b, trace 5) could not be determined because fibrillation was completely inhibited. The slight increase in the fluorescence intensity from a [CdTe]/[$A\beta_{1\text{-}40}$] molar ratio of 0.05 can be most likely ascribed to the formation of NP–peptide agglomerates, the structure of which will be presented later. The slope of the sigmoidal curve is proportional to the elongation rate and also rapidly declines with the amount of NPs. These findings show that both nucleation and growth of fibrils were considerably inhibited by CdTe NPs. Overall, the CdTe NP amounts two to three orders of magnitude smaller than that of the peptide were sufficient to inhibit $A\beta_{1\text{-}40}$ fibrillation. Comparatively, in the case of small molecules and short-peptide inhibitors, the equivalent or an excess amount of the agents is generally required to prevent fibrillation.[1d,4,5,9]

The inhibited fibrillation by CdTe NPs was further confirmed by transmission electron microscopy using the high-angle annular dark field (HAADF) technique (Figure 2). The images show the gradual shortening and disappearance of fibrils as the [CdTe]/[$A\beta_{1\text{-}40}$] ratio increases

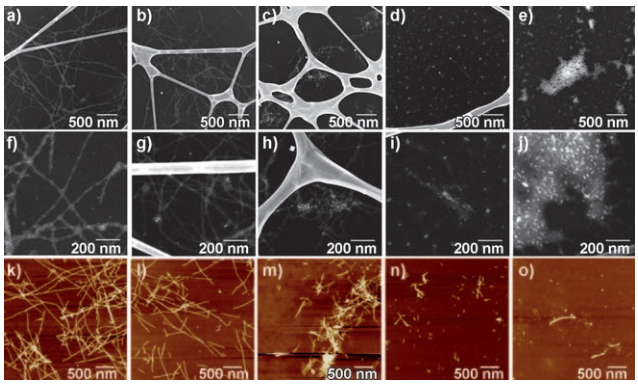

Figure 2. TEM (a–j) and AFM (k–o) images of $A\beta_{1\text{-}40}$ incubated with and without CdTe NPs. [CdTe]/[$A\beta_{1\text{-}40}$] molar ratios: (a,f,k) 0, (b,g,l) 0.001, (c,h,m) 0.005, (d,i,n) 0.01, and (e,j,o) 0.05. In the TEM images, NPs appear as bright spots that can be easily distinguished from the fibrils even for small concentrations of the NPs. Owing to the *Z*-contrast of the images, peptide structures can be visualized directly without staining.

which is confirmed by the fluorescence assay data. All the samples were prepared after the ThT fluorescence had reached a plateau to ensure the visualization of fibrils in equilibrium. In the case of neat $A\beta_{1\text{-}40}$ without CdTe NPs (Figure 2 a,f), $A\beta_{1\text{-}40}$ self-organized into well-defined fibril structures with lengths of more than several micrometers. The diameter of the fibrils varied from around 10 to 40 nm, which can be ascribed to the lateral association of several fibrils.[1] No short fibrils could be found on the entire TEM grid which is indicative of full fibrillation.

At a [CdTe]/[$A\beta_{1\text{-}40}$] molar ratio of 0.005 (Figure 2c,h), the fibrils became considerably shorter with an average length of about 400 nm; bright spots of the NPs can be seen inside the fibrils. A further increase in the molar ratio resulted in additional inhibition of fibril formation. At a [CdTe]/[$A\beta_{1\text{-}40}$] molar ratio of 0.01 (Figure 2d,i), pseudospherical aggregation was mainly observed, although we still found short fibril-like aggregates which incorporated NPs shorter than 100 nm. The fairly large diameter (ca. 18 nm) of the spherical aggregates in the images indicated that individual CdTe NPs (ca. 3.5 nm) were covered with a thick layer of peptide molecules. No uncoated NPs were observed and often more than one NP was included in the larger spherical agglomerates (see Figure S1 in the Supporting Information). Considering [CdTe]/[$A\beta_{1\text{-}40}$] = 0.01 as a threshold for inhibition of fibrillation, we can estimate that one NP binds at least 100 monomers.

When the molar ratio of [CdTe]/[$A\beta_{1\text{-}40}$] reached 0.05, we could not find any indication of fibril formation (Figure 2e,j) and all the particles and peptides formed spherical aggregates. The detailed structures of the NP–peptide aggregates were further examined by high-resolution (HR) TEM analysis, which clearly showed the lattice structure of the NPs inside the agglomerates (see Figure S1 in the Supporting Information). AFM results confirm an effect of the NPs on the self-organization of $A\beta_{1\text{-}40}$. Exactly the same conclusions about the drastic shortening of the fibrils and the dominant formation of spherical agglomerates at a [CdTe]/[$A\beta_{1\text{-}40}$] threshold of 0.01 can be reached by analyzing Figure 2k–o. From the diameter of the spheroid obtained from both TEM and AFM data, we can also calculate that about 330 $A\beta_{1\text{-}40}$ monomers are bound in one spheroid (see Figures S2 and S3 in the Supporting Information for details). Since the TEM data indicate that some spheroids can contain two to three NPs, this number matches quite well with the estimate obtained above.

Subsequently it is important 1) to rationalize why the NPs that we use here give results different from those in the studies conducted before with other NPs[12] and 2) to understand better the mechanism, which might be different from those discussed previously.[12,14] Monomeric $A\beta_{1\text{-}40}$ initially self-associates into disorganized oligomers which then further assemble into β-structured aggregates termed protofibrils.[1,4,14a] There is a kinetic equilibrium among monomers, oligomers, and protofibrils.[1,4,14a] Once the protofibrils are formed, they can act as templates for the further growth of fibrils by allowing rapid association of both monomers and protofibrils, resulting in the sigmoidal growth observed in the ThT assay (Figure 1b). NPs can potentially interfere at any stage of this process. For instance, concomitant studies that involved molecular modeling of peptide packing around CdTe NPs suggest that the association of individual peptides with NPs through a thiol bond or hydrogen bonding result in scrambling of monomeric peptides (see Figure S2 in the Supporting Information).

The interactions of NPs with $A\beta_{1\text{-}40}$ and the inhibition processes were investigated by several complementary microscopy and spectroscopy techniques. SOFAST-HMQC NMR spectra (SOFAST-HMQC = band-selective optimized flip-angle short transient heteronuclear multiple quantum coherence) of ^{15}N-labeled $A\beta_{1\text{-}40}$ were obtained for [CdTe]/[$A\beta_{1\text{-}40}$] molar ratios of 0.0, 0.001, 0.005, 0.01, and 0.05 (Figure 3a). Conditions were intentionally used under which dissolved $A\beta_{1\text{-}40}$ is primarily monomeric and stable (see the Experimental Section). The intensity of the NMR spectra was unchanged for many weeks which is indicative of negligible conversion of the monomer species to larger aggregates.[17] Since the observable peaks in the NMR spectra arise exclusively from the $A\beta_{1\text{-}40}$ monomer,[17] perturbations in the NMR spectra upon addition of CdTe NPs provide a sensitive test for the interaction of CdTe NPs with $A\beta_{1\text{-}40}$ monomers. Interestingly, significant changes in the chemical shifts were not observed for any residues upon addition of CdTe NPs (Figure 3a). While the long rotational correlation time of the $A\beta_{1\text{-}40}$–CdTe NP complex most likely broadens the signal of the complex beyond detection, the equilibrium between the $A\beta_{1\text{-}40}$–CdTe NP complex and the $A\beta_{1\text{-}40}$ monomer can be monitored by measuring the signal intensity and line width, which are reflective of the exchange rate between the monomer and the $A\beta_{1\text{-}40}$–CdTe NP complex. Changes in the line width, suggestive of chemical exchange on the micro- to millisecond timescale, were not observed after addition of CdTe NPs. The intensities of the signals were practically unaffected by the presence of CdTe NPs, as well. Only a slight and mostly uniform decrease in the signal intensity (ca. 20%) was observed as the concentration of CdTe NPs increased (Figure 3b), setting an upper bound on the degree of the depletion of the monomer concentration by the NPs. The lack of a significant interaction of CdTe NPs with the $A\beta_{1\text{-}40}$ monomer indicates that depletion of the monomeric pepti-

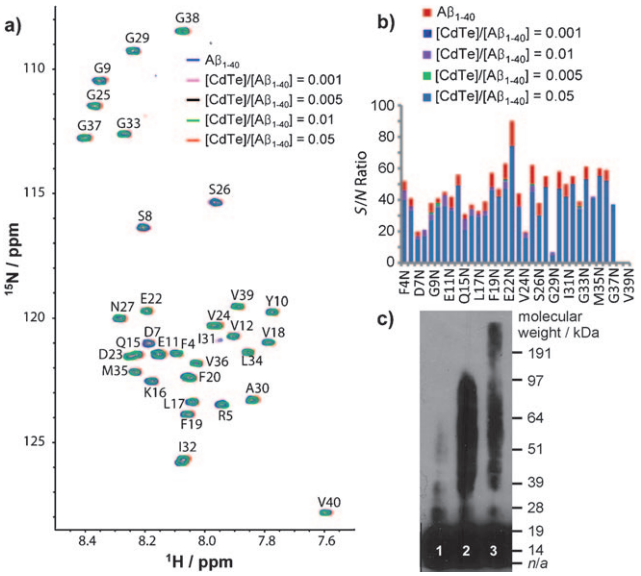

Figure 3. a,b) NMR spectra and c) Western blot with and without CdTe NPs. a) 2D SOFAST-HMQC spectra of freshly dissolved $A\beta_{1\text{-}40}$ with increasing amounts of CdTe NPs at 10°C; b) the change in the signal-to-noise ratio of ^{15}N-labeled $A\beta_{1\text{-}40}$; c) Western blot analysis of freshly prepared $A\beta_{1\text{-}42}$ (lane 1) and $A\beta_{1\text{-}42}$ incubated one day in the absence (lane 2) and presence (lane 3) of CdTe NPs; [CdTe]/[$A\beta_{1\text{-}42}$] = 0.05. Notations for the one-letter abbreviations of the residues can be found in the Supporting Information.

de[14a] is not a likely source for the strong inhibition of $A\beta_{1\text{-}40}$ fibrillation observed in Figures 1 and 2.

The NMR, AFM, TEM, and fluorescence spectroscopy data suggest that the formation of the $A\beta_{1\text{-}40}$–CdTe NP spheroids (Figure 2) is due to the association of oligomers rather than monomers with NPs. This fact can be further confirmed by Western blot analysis (Figure 3c). The freshly dissolved peptide consists mainly of monomers (Figure 3c, lane 1) which aggregate into $A\beta_{1\text{-}42}$ oligomers with a molecular weight of up to around 100 kDa (Figure 3c, lane 2) after incubation. When the same process occurred in the presence of CdTe NPs, the oligomeric bands became noticeably weaker but considerably extended above 100 kDa (Figure 3c, lane 3). Since the molecular weight of the CdTe NP with a diameter of 3.5 nm can be estimated at about 80 kDa, the extended band indicates the binding of CdTe NPs to oligomers.

The distinction between binding to oligomers and monomers as the mechanism of inhibition is quite significant for several reasons: first of all, the difference between binding modalities gives a marked difference in the efficiency of inhibiting fibrillation. Second, the oligomers represent the most neurotoxic species among the $A\beta_{1\text{-}40}$ agglomerates and their blocking by NP complexes is expected to have a great biological effect.[1,3]

To understand better the molecular reasons for the preferential binding of NPs to oligomers and not to monomers, it is instructive to discuss the interactions between them that may include hydrophobic, electrostatic, and van der Waals interactions as well as hydrogen bonding.[15] Hydrophobic interactions between the monomers are known to be the reason for the oligomerization of the peptide.[1,3a,4] These interactions certainly play a role in the stabilization of NP–$A\beta_{1\text{-}40}$ spheroids; however, the hydrophobic forces between NPs and oligomers cannot be strong because the TGA coating is highly hydrophilic.[18] Interestingly, electrostatic interactions are actually acting against the association of NPs and peptides because they are both negatively charged, with zeta potentials of −31.2 and −16.0 mV, respectively. To investigate the hydrogen bonding which can potentially be the driving force for the assembly[14e] infrared (IR) spectra were recorded for a solution of $A\beta_{1\text{-}42}$ after incubation with and without CdTe NPs for one day (Figure 4a). The vibrational bands of the TGA on the NPs, such as the COO^- stretching vibrations at 1585 and 1406 cm^{-1}, and the bands of the peptide, such as the amide I band (C=O stretching vibration) at 1670 cm^{-1} and the amide II band (N−H bending vibration) at 1551 cm^{-1}, remain remarkably unchanged in the NP–oligomer complex (in Figure 4a the band at 1670 cm^{-1} is slightly shifted to 1659 cm^{-1}). The N−H stretching band, which is attributed to NH_2 groups in peptides, also remains at 3323 cm^{-1} in the $A\beta_{1\text{-}42}$ peptide alone and at 3313 cm^{-1} in the CdTe–$A\beta_{1\text{-}42}$ system at a [CdTe]/[$A\beta_{1\text{-}42}$] molar ratio of 0.05. Importantly, no considerable broadening or peak shift typical of any bands that might be responsible for hydrogen-bonding interactions between peptides and NPs, in particular, for COOH groups in the TGA on the NP surface can be observed.[19] Overall, we do not see sufficient IR evidence of extensive hydrogen bonding between NPs and peptide molecules. The same conclusion can also be reached based on NMR spectra

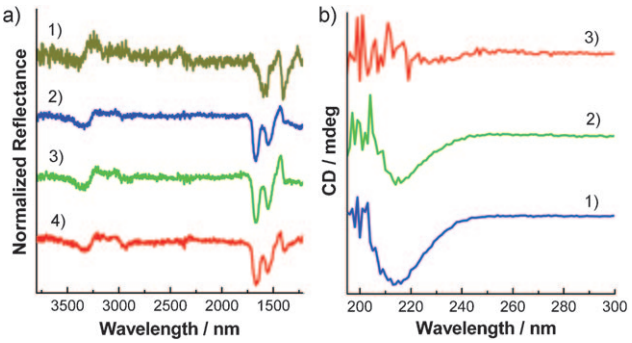

Figure 4. a) FTIR spectra of $A\beta_{1\text{-}42}$ with and without CdTe NPs. 1) CdTe NPs, 2–4) $A\beta_{1\text{-}42}$ with CdTe NPs. [CdTe]/[$A\beta_{1\text{-}42}$] molar ratios: 2) 0, 3) 0.01, and 4) 0.05. b) CD spectra of $A\beta_{1\text{-}42}$ with and without CdTe NPs. [CdTe]/[$A\beta_{1\text{-}42}$] molar ratios: 1) 0, 2) 0.01, and 3) 0.05. Both FTIR and CD spectra were obtained after one day of incubation. In Figure 4b trace 3), the CD signal below 215 nm became noisy by the strong absorbance of the CdTe NPs.

because hydrogen bonding between monomers and NPs must strongly shift the peak positions and coupling constants for the same groups. Considering that there is already strong H bonding in the oligomers, we suggest that the TGA molecules likely have difficulties in competing with these H bonds which are strengthened by a specific conformation of the peptide.

The conundrum behind the formation of NP–oligomer complexes can be explained by the presence of strong van der Waals interactions. They are nonspecific, short-range, but powerful interactions scaling with the molecular weight of the interacting species. The latter feature can explain a number of observations in the context of this and other studies. The preferential binding of NPs to oligomers (Figures 2 and 3) and their negligible association to monomers (Figure 3a,b) are a direct consequence of the fact that van der Waals forces are much stronger between NPs and $A\beta_{1\text{-}40}$ oligomers than among the NPs and monomers. Also, the powerful van der Waals interactions associated with high electron density of atoms in the CdTe–NPs differentiate them from organic nanoparticles studied before[12b,14a–d] and, therefore, provide the atomic basis for the dissimilar effect on fibrillation. The energy of the van der Waals interaction of Aβ with CdTe NPs is as much as 3.5 times higher than that with typical organic NPs (see the Supporting Information for details), and so, instead of accelerating the self-assembly of peptides by a condensation-ordering mechanism,[12] they inhibit self-assembly by immobilizing oligomers in the spheroids around the NPs. Also note: CdTe NPs are tetrahedral and comparable in size to the peptide (Figure 1a). Strong attraction between elongated oligomers/protofibrils and NPs will result in their "wrapping" around the edges of the semiconductor core and concomitant distortion of the amyloid pattern. To verify this we examined the secondary structure of the oligomers after formation of spheroids by circular dichroism (CD) spectroscopy which is very sensitive to conformational changes. $A\beta_{1\text{-}42}$ oligomers displayed one negative peak at 215 nm corresponding to β-sheet packing of the peptides.[20] The peak completely disappeared with the addition of CdTe NPs (Figure 4b) which is indicative of scrambling of peptide chains.

It is also instructive to compare this inhibitory activity of CdTe NPs to that of proteins known for their protective function against AD. Human serum albumin (HSA) is one of the most potent endogenous inhibitors of amyloid fibrillation; it acts as an "external sink" and does not need to cross the blood–brain barrier. HSA forms complexes with Aβ oligomers but does not interact appreciably with monomers.[6a,b] One HSA protein associates with approximately 20 monomers and a [HSA]/[Aβ] ratio of about 0.056 effectively prevents fibrillation.[6a] This ratio is substantially larger than the ratio observed for the NPs (Figures 1 and 2). HSA is much more efficient than regular small AD drugs that are typically effective in the equivalent or an excess ratio (i.e., [small drug]/[Aβ] ≥ 1) and made to bind peptide monomers. Unlike NPs, however, HSA takes advantage of mostly hydrophobic interactions and binds to the exposed hydrophobic domain of the oligomers, while other interactions play mostly a secondary role. The size of HSA is about 3.3 nm,[21] which is slightly larger than the CdTe NPs used here. Another inhibitory protein, apolipoprotein E3 (apoE3), prevents fibrillation at a [apoE3]/[Aβ] ratio of 0.001.[6d] The mechanism is associated with binding to disorganized (prenucleus) oligomers and not to monomers; immobilization of the oligomer in this state prevents their further crystallization, which is analogous to that proposed here for the NPs. The nature of interactions between apoE3 and Aβ is not known.

Overall, it is quite clear that the mechanism of fibril inhibition exerted by CdTe NPs is surprisingly similar to that of proteins, although the actions arise from different intermolecular interactions. Despite the fact that CdTe NPs are cytotoxic and cannot be used in vivo, this model demonstrates that NPs can reach equal or better efficiency of fibrillation inhibition than the best-known proteins. This work also offers a blueprint for the nanoscale engineering of NPs from biocompatible materials with similar properties. Biocompatible NP systems mimicking the structural characteristics of CdTe NPs, particularly those with a sharp faceted structure, can be suggested to replace toxic CdTe NPs for inhibiting amyloid fibrillation.

Experimental Section

$A\beta_{1\text{-}40}$ was purchased from Invitrogen and was used as received. A stock solution of $A\beta_{1\text{-}40}$ was typically prepared by dissolving the lyophilized peptide in dimethyl sulfoxide (DMSO) to a final concentration of 1 mM. For the fibrillation, the stock solution of $A\beta_{1\text{-}40}$ was added to phosphate-buffered saline (PBS buffer, pH 7.4) to yield a 25 μM $A\beta_{1\text{-}40}$ solution. Thioglycolic acid (TGA)-stabilized CdTe NPs were prepared as previously reported.[15] UV/Vis and fluorescence spectra of CdTe NPs are shown in Figure S4 in the Supporting Information, and they varied slightly with each synthesis. From the UV/Vis absorption spectra the size of NPs was estimated to about 3.5 nm.[22]

To investigate the influence of CdTe NPs on the fibrillation of $A\beta_{1\text{-}40}$, different amounts of CdTe NPs were added to the incubation solutions. The molar ratio of CdTe NPs to $A\beta_{1\text{-}40}$ was adjusted to 0, 0.001, 0.005, 0.01, and 0.05. Then the incubation solutions with and without CdTe NPs were stirred at room temperature typically for one day. The fibrillation of $A\beta_{1\text{-}40}$ by a ThT assay was also monitored after addition of a stock solution of $A\beta_{1\text{-}40}$ and CdTe NPs to 20 μM ThT solution in PBS buffer. Photoluminescence spectra of the ThT assay were recorded using a Fluoromax-3 spectrofluorometer (Jobin Yvon/SPEX Horiba, NJ) with an excitation wavelength of 450 nm and a monitoring wavelength of 485 nm.

The morphology of $A\beta_{1\text{-}40}$ with and without CdTe NPs was studied with a transmission electron microscope (JEOL 2010F) operated in the scanning transmission electron microscopy (STEM) mode. Atomic force microscopy (AFM) imaging was performed with a Nanoscope III (Digital Instruments/Veeco Metrology Group). For the AFM measurement, lyophilized $A\beta_{1\text{-}40}$ was first dissolved in deionized water and then diluted in PBS buffer with and without NPs.

NMR samples were prepared from ^{15}N-labeled $A\beta_{1\text{-}40}$ (rPeptide) by first dissolving the peptide in 1% ammonium hydroxide, lyophilizing, and then resuspending in DMSO to a 1 mM peptide concentration. The peptide was then diluted to a final concentration of 76.6 μM in 20 mM sodium phosphate buffer, pH 7.5, with 50 mM NaCl. All NMR experiments were performed on a Bruker spectrometer operating at 600.13 MHz (^1H NMR frequency), equipped with a cryogenic probe. The interactions of $A\beta_{1\text{-}40}$ with CdTe NPs were followed by performing a series of 2D SOFAST-HMQC experiments[23] at 10 °C with increasing concentrations of CdTe NPs. Each spectrum was obtained from 128 t_1 experiments, four scans, and a 100 ms recycle delay (t_1 = incremental delay in the 2D experiment). The final 2D data matrix size was 2048 × 2048 after zero-filling in both dimensions. 2D data were processed using TOPSPIN 2.1 (from Bruker). A squared sine-bell function was employed in both dimension with a shift of π/4. Resonance assignment and volume fit calculations were performed using SPARKY 3.113.

Received: December 12, 2010
Published online: April 14, 2011

Keywords: fibrils · nanoparticles · peptides · self-assembly

[1] a) F. Chiti, C. M. Dobson, *Annu. Rev. Biochem.* **2006**, *75*, 333; b) P. T. Lansbury, H. A. Lashuel, *Nature* **2006**, *443*, 774; c) C. A. Ross, M. A. Poirier, *Nat. Rev. Mol. Cell Biol.* **2005**, *6*, 891; d) J. Hardy, D. J. Selkoe, *Science* **2002**, *297*, 353.

[2] a) A. T. Petkova, R. D. Leapman, Z. Guo, W.-M. Yau, M. P. Mattson, R. Tycko, *Science* **2005**, *307*, 262; b) A. Lorenzo, B. A. Yankner, *Proc. Natl. Acad. Sci. USA* **1994**, *91*, 12243.

[3] a) C. Haass, D. J. Selkoe, *Nat. Rev. Mol. Cell Biol.* **2007**, *8*, 101; b) J. P. Cleary, D. M. Walsh, J. J. Hofmeister, G. M. Shankar, M. A. Kuskowski, D. J. Selkoe, K. H. Ashe, *Nat. Neurosci.* **2004**, *8*, 79; c) G. Bitan, M. D. Kirkitadze, A. Lomakin, S. S. Vollers, G. B. Benedek, D. B. Teplow, *Proc. Natl. Acad. Sci. USA* **2003**, *100*, 330; d) D. M. Walsh, I. Klyubin, J. V. Fadeeva, W. K. Cullen, R. Anwyl, M. S. Wolfe, M. J. Rowan, D. J. Selkoe, *Nature* **2002**, *416*, 535; e) W. L. Klein, G. A. Krafft, C. E. Finch, *Trends Neurosci.* **2001**, *24*, 219.

[4] T. Takahashi, H. Mihara, *Acc. Chem. Res.* **2008**, *41*, 1309.

[5] a) D. J. Gordon, K. L. Sciarretta, S. C. Meredith, *Biochemistry* **2001**, *40*, 8237; b) T. L. Lowe, A. Strzelec, L. L. Kiessling, R. M. Murphy, *Biochemistry* **2001**, *40*, 7882; c) M. A. Findeis, G. M. Musso, C. C. Arico-Muendel, H. W. Benjamin, A. M. Hundal, J.-J. Lee, J. Chin, M. Kelley, J. Wakefield, N. J. Hayward, S. M. Molineaux, *Biochemistry* **1999**, *38*, 6791; d) L. O. Tjernberg, J. Näslund, F. Lindqvist, J. Johansson, A. R. Karlström, J. Thyberg, L. Terenius, C. Nordstedt, *J. Biol. Chem.* **1996**, *271*, 8545; e) C. Soto, M. S. Kindy, M. Baumann, B. Frangione, *Biochem. Biophys. Res. Commun.* **1996**, *226*, 672.

[6] a) J. Milojevic, A. Raditsis, G. Melacini, *Biophys. J.* **2009**, *97*, 2585; b) J. Milojevic, V. Esposito, R. Das, G. Melacini, *J. Am. Chem. Soc.* **2007**, *129*, 4282; c) B. Bohrmann, L. Tjernberg, P. Kuner, S. Poli, B. Levet-Trafit, J. Näslund, G. Richards, W. Huber, H. Döbeli, C. Nordstedt, *J. Biol. Chem.* **1999**, *274*, 15990;

d) K. C. Evans, E. P. Berger, C.-G. Cho, K. H. Weisgraber, *Proc. Natl. Acad. Sci. USA* **1995**, *92*, 763.
[7] a) I. Klyubin, D. M. Walsh, C. A. Lemere, W. K. Cullen, G. M. Shankar, V. Betts, E. T. Spooner, L. Jiang, R. Anwyl, D. J. Selkoe, M. J. Rowan, *Nat. Med.* **2005**, *11*, 556; b) C. Hock, U. Konietzko, A. Papassotiropoulos, A. Wollmer, J. Streffer, R. C. von Rotz, G. Davey, E. Moritz, R. M. Nitsch, *Nat. Med.* **2002**, *8*, 1270.
[8] J. F. Poduslo, G. L. Curran, C. T. Berg, *Proc. Natl. Acad. Sci. USA* **1994**, *91*, 5705.
[9] M. A. Findeis, *Biochim. Biophys. Acta Mol. Basis Dis.* **2000**, *1502*, 76.
[10] a) Y. Bae, N. H. Kim, M. Kim, K. Y. Lee, S. W. Han, *J. Am. Chem. Soc.* **2008**, *130*, 5432; b) G. A. DeVries, Y. Hu, B. Long, B. T. Neltner, O. Uzun, B. H. Wunsch, F. Stellacci, *Science* **2007**, *315*, 358; c) M. Klokkenburg, A. J. Houtepen, R. Koole, J. W. J. de Folter, B. H. Erné, E. van Faassen, D. Vanmaekelbergh, *Nano Lett.* **2007**, *7*, 2931; d) S.-H. Yu, H. Cölfen, K. Tauer, M. Antonietti, *Nat. Mater.* **2005**, *4*, 51; e) K.-S. Cho, D. V. Talapin, W. Gaschler, C. B. Murray, *J. Am. Chem. Soc.* **2005**, *127*, 7140; f) W. Lu, P. Gao, W. B. Jian, Z. L. Wang, J. Fang, *J. Am. Chem. Soc.* **2004**, *126*, 14816; g) Z. Y. Tang, N. A. Kotov, M. Giersig, *Science* **2002**, *297*, 237.
[11] a) Y. Xia, *Nat. Mater.* **2008**, *7*, 758; b) I. Lynch, K. A. Dawson, *Nano Today* **2008**, *3*, 40; c) M. Sarikaya, C. Tamerler, A. K. Y. Jen, K. Schulten, F. Baneyx, *Nat. Mater.* **2003**, *2*, 577.
[12] a) S. Auer, A. Trovato, M. A. Vendruscolo, *Plos Comput. Biol.* **2009**, *5*, e1000458; b) S. Linse, C. Cabaleiro-Lago, W.-F. Xue, I. Lynch, S. Lindman, E. Thulin, S. E. Radford, K. A. Dawson, *Proc. Natl. Acad. Sci. USA* **2007**, *104*, 8691; c) W. H. Wu, X. Sun, Y. P. Yu, J. Hu, L. Zhao, Q. Liu, Y. F. Zhao, Y. M. Li, *Biochem. Biophys. Res. Commun.* **2008**, *373*, 315.
[13] a) A. Relini, C. Canale, S. De Stefano, R. Rolandi, S. Giorgetti, M. Stoppini, A. Rossi, F. Fogolari, A. Corazza, G. Esposito, A. Gliozzi, V. Bellotti, *J. Biol. Chem.* **2006**, *281*, 16521; b) S. L. Myers, S. Jones, T. R. Jahn, I. J. Morten, G. A. Tennent, E. W. Hewitt, S. E. Radford, *Biochemistry* **2006**, *45*, 2311; c) V. Sluzky, J. A. Tamada, A. M. Klibanov, R. Langer, *Proc. Natl. Acad. Sci. USA* **1991**, *88*, 9377; d) J. R. Lu, S. Perumal, E. T. Powers, J. W. Kelly, J. R. P. Webster, J. Penfold, *J. Am. Chem. Soc.* **2003**, *125*, 3751; e) E. T. Powers, J. W. Kelly, *J. Am. Chem. Soc.* **2001**, *123*, 775.
[14] a) C. Cabaleiro-Lago, F. Quinlan-Pluck, I. Lynch, S. Lindman, A. M. Minogue, E. Thulin, D. M. Walsh, K. A. Dawson, S. Linse, *J. Am. Chem. Soc.* **2008**, *130*, 15437; b) K. Ikeda, T. Okada, S.-I. Sawada, K. Akiyoshi, K. Matsuzaki, *FEBS Lett.* **2006**, *580*, 6587; c) A. S. Pai, I. Rubinstein, H. Onyüksel, *Peptides* **2006**, *27*, 2858; d) J. E. Kim, M. Lee, *Biochem. Biophys. Res. Commun.* **2003**, *303*, 576; e) L. Xiao, D. Zhao, W.-H. Chan, M. M. F. Choi, H.-W. Li, *Biomaterials* **2010**, *31*, 91.
[15] a) Z. Tang, Z. Zhang, Y. Wang, S. C. Glotzer, N. A. Kotov, *Science* **2006**, *314*, 274; b) Z. Zhang, Z. Tang, N. A. Kotov, S. C. Glotzer, *Nano Lett.* **2007**, *7*, 1670.
[16] The fitting curves were obtained from an equation in Ref. [14], $y = y_0 + (y_{max} - y_0)/(1 + e^{-(t-t_{1/2})k})$, where y is the fluorescence intensity at a given time t, y_0 and y_{max} are the initial and maximum fluorescence intensity, respectively, $t_{1/2}$ is the time required to reach half of the maximum fluorescence intensity, and k is the apparent first-order aggregation constant. The lag time can be calculated by $t_{1/2} - 2/k$. Since the fibrillation was completely inhibited in the case of $[CdTe]/[A\beta_{1\text{-}40}] = 0.05$, we were not able to include a fitting curve. The solid line in Figure 1 b, trace 5 is a guide to the eye.
[17] N. L. Fawzi, J. Ying, D. A. Torchia, G. M. Clore, *J. Am. Chem. Soc.* **2010**, *132*, 9948.
[18] A. A. Yaroslavov, V. A. Sinani, A. A. Efimova, E. G. Yaroslavova, A. A. Rakhnyanskaya, Y. A. Ermakov, N. A. Kotov, *J. Am. Chem. Soc.* **2005**, *127*, 7322.
[19] a) Q. Shang, H. Wang, H. Yu, G. Shan, R. Yan, *Colloids Surf. A* **2007**, *294*, 86; b) Z. Li, Y. Du, Z. Zhang, D. Pang, *React. Funct. Polym.* **2003**, *55*, 35.
[20] P. Manavalan, W. C. Johnson, *Nature* **1983**, *305*, 831.
[21] J. R. Olivieri, A. F. Craievich, *Eur. Biophys. J.* **1995**, *24*, 77.
[22] W. W. Yu, L. Qu, W. Guo, X. Peng, *Chem. Mater.* **2003**, *15*, 2854.
[23] P. Schanda, B. Brutscher, *J. Am. Chem. Soc.* **2005**, *127*, 8014.

